Draft version February 19, 2015
Preprint typeset using LaTeX style emulateapj v. 05/12/14

arXiv:1502.05270v1 [astro-ph.HE] 18 Feb 2015

TOWARD AN EMPIRICAL THEORY OF PULSAR EMISSION XI. UNDERSTANDING THE ORIENTATIONS OF PULSAR RADIATION AND SUPERNOVA "KICKS"

Joanna M. Rankin
Physics Department, University of Vermont, Burlington, VT 05405 USA:
Joanna.Rankin@uvm.edu

Draft version February 19, 2015

ABSTRACT

Two entwined problems have remained unresolved since pulsars were discovered nearly 50 years ago: the orientation of their polarized emission relative to the emitting magnetic field and the direction of putative supernova "kicks' relative to their rotation axes. The rotational orientation of most pulsars can be inferred only from the ("fiducial') polarization angle of their radiation, when their beam points directly at the Earth and the emitting polar fluxtube field is ∥ to the rotation axis. Earlier studies have been unrevealing owing to the admixture of different types of radiation (core and conal, two polarization modes), producing both ∥ or ⊥ alignments. In this paper we analyze the some 50 pulsars having three characteristics: core radiation beams, reliable absolute polarimetry, and accurate proper motions. The "fiducial' polarization angle of the core emission, we then find, is usually oriented ⊥ to the proper-motion direction on the sky. As the primary core emission is polarized ⊥ to the projected magnetic field in Vela and other pulsars where X-ray imaging reveals the orientation, this shows that the proper motions usually lie ∥ to the rotation axes on the sky. Two key physical consequences then follow: first, to the extent that supernova "kicks' are responsible for pulsar proper motions, they are mostly ∥ to the rotation axis; and second that most pulsar radiation is heavily processed by the magnetospheric plasma such that the lowest altitude "parent' core emission is polarized ⊥ to the emitting field, propagating as the extraordinary (X) mode.

Keywords: pulsars: general — techniques: polarimetric; emission mechanisms: non-thermal

1. INTRODUCTION

Radio pulsars now contribute importantly to many fields of physical science, but paradoxically, two fundamental coupled issues have remained unresolved since they were discovered 47 years ago: the orientation of their linearly polarized emission relative to the magnetic field in their polar fluxtube emitting regions and the origin/orientation of their often large space velocities (and thus proper motions) relative to their rotation axes. Most pulsars are known only by their lighthouse-like radio signals, and thus we have no direct means of determining the orientation of a pulsar's rotation axis on the sky, which is crucial both to interpreting the polarization direction of the radiation and the orientation of the proper motion relative to the spin axis. Pulsars radiate because highly energetic outward-going charges are accelerated by the curved dipolar field within their polar regions, so it is crucial to understand how this radiation is polarized relative to the (projected) **B** field orientation on the sky. Figure 1 shows how this field appears splayed when a pulsar's beam points directly at the Earth—the "fiducial" instant—and that the emission reaching us is associated with that bundle in the plane of the rotation axis **Ω**. Clearly, we have no knowledge of the radial component of a pulsar's space velocity and only weak estimates of the radial component of **Ω**.

At one time it seemed obvious that pulsar radiation must be polarized ∥ to the projected magnetic field direction. How could it be otherwise given that both the curving **B** field and the resulting curvature acceleration lie in the same plane? Even after the discovery that pulsars emit in two orthogonal (hereafter OPM) polarization modes [Backer & Rankin (1980); Manchester et al. (1975)] many assumed in the absence of any direct proof that the "primary" polarization mode must be ∥.

This easy presumption was dashed in the new millennium by X-ray imaging of the Vela pulsar [Helfand et al. (2001); Radhakrishnan & Deshpande (2001)] where arcs indicated the orientation of the star's rotation axis **Ω** relative to its polarization and proper-motion (PM) directions. Shockingly, the radiation was polarized ⊥ to the projected magnetic field **B** plane, a circumstance then beautifully confirmed for the radio emission (Johnston et al. 2005, hereafter Johnston I)—and this pulsar's radio emission is almost completely linearly polarized, so there was no OPM ambiguity.

In an earlier paper (Rankin 2007, hereafter Paper I) we investigated the PPA vs. PM alignments of a number of pulsars, drawing strongly on Johnston I as well as other sources. Here, a "fiducial" polarization position angle (PPA) PA_0, at a ("fiducial") rotational phase representing the magnetic axis longitude, is measured and referred to infinite frequency as a proxy for the (unseen) orientation of the rotation axis **Ω**. These were compared with well determined proper-motion (PM) directions PA_V, and the differences Ψ showed strong peaks at both 0° and 90°. Given, however, that most of the pulsars showed strong OPM activity in their profiles, it was not possible to draw general conclusions about the polarization orientation with respect to the projected **B** direction.

The second coupled key question is how a pulsar's rotation vector **Ω** is oriented with respect to its space velocity (of which we can usually measure only their projections on the plane of the sky)? The possibility of a cor-

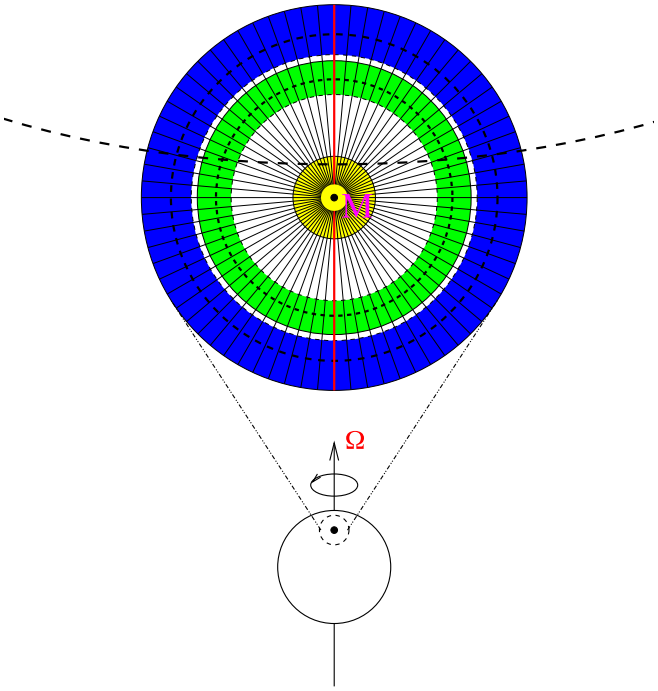


Figure 1. Diagram showing the splayed curving field lines—here shown in projection—associated with pulsar emission at the "fiducial" instant when the beam faces the Earth directly. Both the magnetic axis **M** and pulsar rotation axis **Ω** are indicated in relation to the "fiducial" field lines (magneta) associated with the radiation we receive at that instant. The projected fiducial field is ∥ to the rotation axis **Ω** and thus used as a proxy for **Ω** which is otherwise usually not observable. Also indicated is the emission-beam structure consisting of two concentric conal beams (outer: blue and inner: green) and the central core beam (yellow) in relation to a typical sightline traverse (black dashed). Any of the three beams can be present in a given pulsar and different sightline paths result in different profile types. Profiles with a core beam are of primary interest here—that is, the core-single (**S**$_t$) where it appears on its own; triple (**T**) profiles where one of the cones is present; and five-component (**M**) profiles where both cones appear.

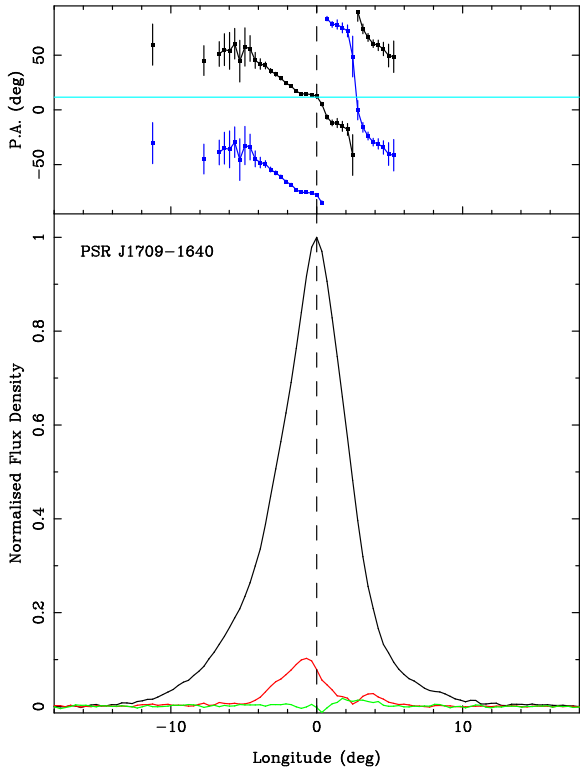


Figure 2. Polarization profile of B1706–16 from Johnston I showing its highly depolarized single core-component profile at 1369 MHz. The roughly linear, negative-going PPA (black curve) plotted in the upper panel connects smoothly with the PPA − 90° (blue) curve on the trailing edge of the profile, coinciding with the minimum in the linear polarization (red curve) in the lower panel where the total power (black) and circular polarization (green) are also plotted. The PPAs are referred to infinite frequency, and the PA_V value is shown as a horizontal (cyan) line. See text.

relation was raised early [Shklovskii (1969); Gott et al. (1970); Tademaru & Harrison (1975)] as their large peculiar velocities were realized, initially through scintillation studies. Though no binary pulsar was then known, their presumptive birth in the disruption of such systems appeared to be a significant factor in their PMs. However, binary disruption ultimately seemed inadequate to account for the very large velocities of some pulsars. Theorists then began to explore other mechanisms for their acceleration—in particular the question of whether natal supernovae imparted "kicks" to their progeny.

This "kick" question has a complex history which is nicely summarized in (Noutsos et al. 2012). Suffice it to say that theorists suggested ingenious "kick" mechanisms—both ∥ and ⊥ to the orientation of a pulsar's rotation **Ω** (as well possibly in combination?). Mechanisms such as Galactic acceleration are known which would tend to alter such "birth" alignments (*e.g.*, Noutsos et al. 2013), however the analyses quoted above indicate that a surprisingly large proportion of pulsars show Ψ orientation close to either 0° or 90°. Again, however, the orientation of **Ω** cannot usually be determined directly, but only though the fiducial PPA proxy PA_0 that is complicated by OPM radiation either ∥ or ⊥ to the projected **B** direction. This double ambiguity of proper-motion direction and OPM orientation has plagued efforts to settle how supernovae contribute to pulsar velocities.

Although much of our earlier work had focused on classifying the properties of different pulsar profile populations according primarily to their emission geometry and frequency evolution [Rankin 1983, 1990, 1993a, 1993b; Rankin et al. (1989); Mitra & Rankin (2011); hereafter ET I, IV, VIa,b, — & IX], our analysis in Paper I failed to use this information, despite the fact that most of the stars there under consideration had long been classified through detailed study. Most of the pulsars in the Johnston I study exhibited core, core-cone, or core-double cone profiles of the core-single (**S**$_t$), triple (**T**) or five-component (**M**) types (see Fig. 1), and most of the 90° alignments pertained to pulsars of these types, but this circumstance was not then observed or interpreted.

In large part this failure stemmed from the complexity of the PPA traverses in some pulsars with bright core components. A number exhibit PPA traverses that are readily fitted by the expected rotating-vector (RVM) model (Radhakrishnan & Cooke 1969), while others have depolarized, OPM-active components with distorted PPA traverses that have proven difficult to explain and interpret. Recently, several detailed analyses of particular bright pulsars with prominent core emission

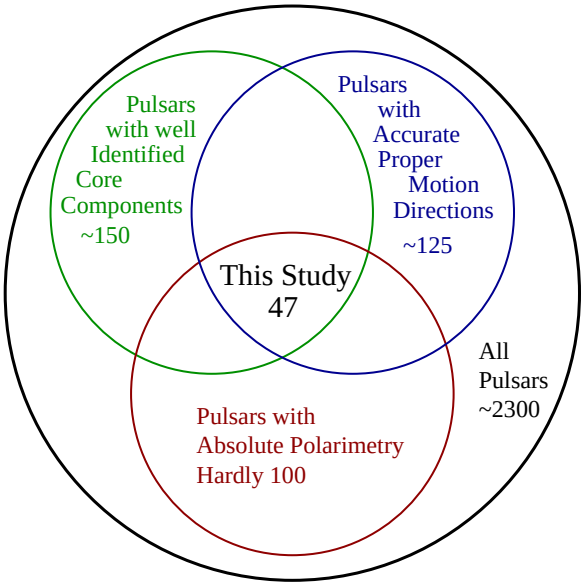


Figure 3. Venn diagram showing the particular population of 47 pulsars having accurate determinations of three different types that is the foundation of this analysis.

have helped us to understand these effects more fully [Mitra et al. (2007); Smith et al. (2013)], and we have found that intensity-dependent aberration/retardation (A/R, see Blaskiewicz et al. 1991)—an effect first seen in the Vela pulsar (Krishnamohan & Downs 1983)—is also a major source of PPA-traverse distortion in cores.

Figure 2 shows a clear case of this sort of depolarization and distortion of an otherwise nearly linear PPA traverse. The emission in the trailing part of the component reflects one OPM and that in the earlier part the other, apparently because more intense fractions of this later "parent" emission appear earlier due to the intensity-dependent A/R and some of it is seemingly converted to the other OPM.

2. THREE OVERLAPPING ANALYSES

The analysis of this paper is based on three different types of pulsar investigation: a) reliable identification of pulsars with central core-beam emission; b) well determined fiducial PPA measurements; and c) accurate proper motion (PM) directions.

Core emission was first distinguished from the conal type in ET I and populations of pulsars with core emission components identified in ET IV, VI & IX. Emission geometry analyses for more than 50 core single ($\mathbf{S}_t$), some 50+ core-cone triple ($\mathbf{T}$) as well as a few core/double-cone ($\mathbf{M}$) stars are given in the tables of ET VIb. This overall core population is key to our analysis below because almost all of these identifications have proven to be accurate, many through further detailed single pulse studies. Moreover, core components usually appear to fall close to the magnetic axis longitude in pulsar profiles, so provide a useful indicator in this regard.

Fiducial polarization angle measurements PA_0 are here used as proxies for the orientation of a pulsar's rotation axis on the sky. First, they require absolute PPA calibration—that is, referenced to an origin measured counter-clockwise from North on the sky—and second, they must be referred to infinite frequency by accurately unwrapping the Faraday rotation of the PPAs. Then the "fiducial" magnetic axis longitude is estimated by PPA-fitting or profile-analysis. Most of the published pulsar polarimetry lacks absolute calibration. The Effelsberg instrument pioneered this work [Morris et al. (1979); Morris et al. (1981); Xilouris et al. (1991)], but important recent efforts have been carried out at Parkes (Johnston I; Karastergiou & Johnston (2006); Johnston et al. (2007), hereafter Johnston II] as well as Arecibo (Paper I) and the GBT [Noutsos et al. (2012); Force et al. (preprint)]—bringing the total to about 100 objects.

Accurate proper-motion directions PA_V, measured CCW from North, are known for just over 100 normal and some 25 millisecond pulsars. Earlier, pulsar PMs were measured reliably only with interferometry, but over the last decade special pulsar-timing methods have also produced useful measurements (Hobbs *et al* 2004, 2005).

In what follows then, we assemble this three-fold information as indicated in Figure 3 on the nearly 50 pulsars having reliable PM directions, absolute fiducial PPA determinations and well identified core-emission components. Table 1 summarizes these proper-motion directions PA_V, proxy rotation-axis orientations PA_0 as well as their differences Ψ. The PA_V references show the origins of these values and in several cases their correction. The PA_0 references trace their origins from Johnston I, Paper I, Johnston II, Force *et al*, and the present study (Tables A1-A5, respectively). Notes to these Appendix tables explain needed revisions or problems. Most classifications remain accurate from ET IV and ET VI, with only a few having been classified anew or reclassified as a result of new information. Similarly, most PA_0 values appeared accurate as determined in the above sources, and where corrections or different interpretations are made, these are described in the table notes.

3. DISCUSSION

The overall distribution of the computed alignment angles Ψ [$= PA_V - PA_0$] for core emission is shown in Figure 4. Each value is represented by a von Mises function of equal area with its standard deviation corresponding to its error. All 47 pulsars currently having the three-fold analysis—that is, accurate proper motions together with fiducial PPAs of relatively well identified core emission—appear in Table 1, the Appendix tables and the above figure.

Clearly, the analysis shows that core emission exhibits a strong orthogonal alignment on the plane of the sky. Most of the Ψ values fall near 90° and often accurately so. Indeed, interpreting Fig. 4 probabilistically, half the weight falls within 90±10°, 2/3 within ±20°and 3/4 within ±30°; only 14% falls within 0±30/degr. We see here that the "fiducial" PPA PA_0 (in several cases computed to track the "parent" core OPM) is usually orthogonal to the proper-motion direction PA_V.

The "fiducial" instant furthermore implies that the projected direction of the emitting magnetic field is in turn ∥ to the rotation axis $\mathbf{\Omega}$ on the sky (see Fig. 1). None of this, however, fixes how the electric vector (defining the linear PPA direction) of the core emission is oriented with respect to the projected magnetic field direction. For this we must refer to X-ray images of Vela and cer-

Table 1
Alignment Angles for Pulsars with Core Components.

Pulsar	PA_V (deg)	Ref.	PA_0 (deg)	Ref.	Ψ (deg)
B0011+47	+136(3)	1	43(7)	A4	–87(8)
B0136+57	–131(0)	2	43(3)	A4	6(3)
B0329+54	119(1)	3	20(4)	A2	99(4)
B0355+54	48(1)	4	–41(4)	A2	89(5)
B0450+55	108(0)	2	–23(16)	A2	–94(16)
B0450–18	40(5)	2	47(3)	A3	–7(6)
B0540+23	58(19)	5	–85(3)	A3	–37(19)
B0628–28	294(2)	1	26(2)	A1	88(3)
B0736–40	227(5)[a]	1	–44(5)	A2	91(7)
B0823+26	146(1)	6	48(3)	A2	98(3)
B0833–45	301(0)	7	37(1)	A1	84(1)
B0835–41	187(6)	1	–84(5)	A3	91(8)
B0919+06	12(0)	8	–77(10)	A1	89(10)
B1237+25	295(0)	3	–28(4)	A1	–37(4)
B1322+83	–76(13)	5	26(3)	A4	78(15)
B1426–66	236(5)	9	–29(1)	A1	84(5)
B1449–64	217(2)	9	–57(0)	A1	94(2)
B1451–68	253(0)	10	–22(4)	A1	95(4)
B1508+55	–130(0)	5	5(4)	A2	45(4)
B1541+09	–111(0)	2	–32(15)	A5	–79(17)
B1600–49	268(6)	9	0(5)	A3	88(8)
B1642–03	353(3)	1	89(8)	A1	84(8)
B1706–16	192(4)	11	–75(2)	A1	87(4)
B1706–44	160(10)	12	71(10)	A1	89(14)
B1732–07	–5(3)	1	–22(1)	A4	17(4)
B1737+13	228(6)	1	–46(4)	A1	94(7)
B1818–04	–22(17)	13	55(3)	A3	–77(17)
B1821–19	–173(17)	14	53(2)	A4	–46(17)
B1826–17	+172(9)	14	11(1)	A4	–19(9)
B1842+14	36(8)	11	–52(2)	A1	88(9)
B1848+13	237(16)	13	–45(3)	A3	–78(16)
B1857–26	203(0)	5	–69(10)	A1	92(10)
B1911–04	166(5)	11	–99(8)	A1	85(9)
B1913+10	174(15)	13	85(3)	A3	89(15)
B1929+10	65(0)	8	–11(0)	A1	77(0)
B1933+16	176(1)	11	–87(1)	A1	89(1)
B1935+25	220(9)	13	–56(8)	A3	96(12)
B1946+35	–93(3)[b]	13	–78(15)	A5	–16(15)
B2045–16	92(2)	15	–13(5)	A3	–75(6)
B2053+36	157(1)	5	–77(11)	A5	54(11)
B2110+27	–157(2)	5	–64(5)	A5	87(5)
B2111+46	–20(44)	13	86(0)	A4	66(44)
B2217+47	–158(10)	6	65(8)	A4	–4411)
B2224+65	+52(1)	5	–48(5)	A4	–80(5)
B2255+58	+106(12)	14	24(3)	A4	82(12)
B2310+42	+76(0)	2	18(10)	A4	58(10)
B2327–20	86(2)	1	21(10)	A3	65(10)

[a]Here we use Brisken et al. (2003) PA_V value rather than the analysis in Johnston *et al* II, correcting the error in Paper I. [b]The origin of the interferometric proper motion value in Hobbs et al. (2005) is unclear, so we have used the timing value in Hobbs *et al* (2004).
Proper-motion references: (1) Brisken et al. (2003), (2) Chatterjee et al. (2009), (3) Brisken et al. (2002), (4) Chatterjee et al. (2005), (5) Harrison et al. (1993), (6)Lyne et al. (1982), (7) Dodson et al. (2003), (8) Chatterjee et al. (2001), (9) Bailes et al. (1990a), (10) Bailes et al. (1990b), (11) Johnston *et al* I updates of Hobbs *et al* (2004), (12) Ng & Romani (2004), (13) Hobbs et al. (2004), (14) Zou et al. (2005), (15) Fomalont et al. (1997)

tain other pulsars (*e.g.*, Helfand *et al* 2001; Ng & Romani 2004) from which the rotation-axis orientation on the sky can be compared with the radio "fiducial" polarization direction of the core emission—and the result that they are again orthogonal.

These circumstances then support several conclusions—

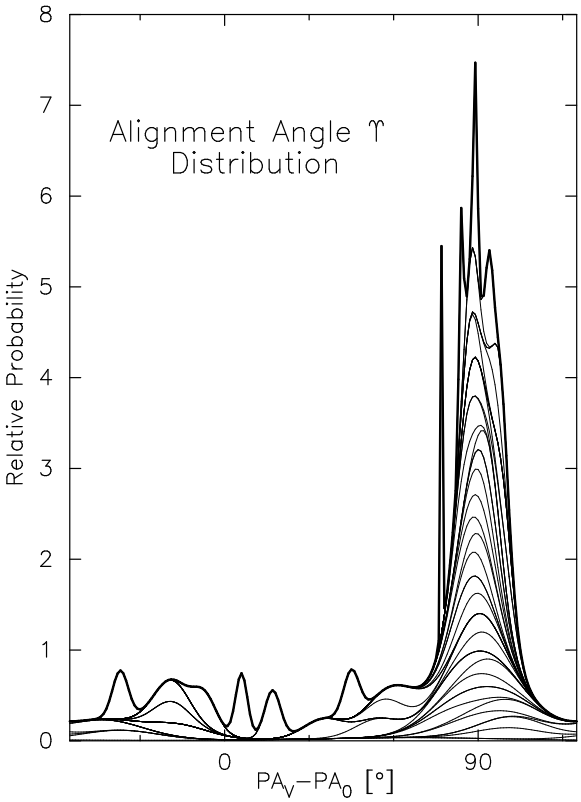


Figure 4. Distribution showing the core-emission alignment angles Ψ of the 47 pulsars in Tables A1 to A5. Here the alignment of each pulsar is represented by a 180°-von Mises function with peak Ψ and standard deviation corresponding to its error value. Each function has equal area such that the total area of the cumulative distribution corresponds to the area of the region below unity.

- Core emission tends to be polarized perpendicularly to the projected magnetic field direction and thus propagates as the extraordinary (X) physical mode. In a few cases we must distinguish the (later or probably lower altitude) "parent" core emission.

- Most pulsar proper motions fall closely ∥ to the magnetic axis direction $\mathbf{\Omega}$. The narrowness of this distribution around 90° is first surprising given the mechanisms that would degrade such alignments, and second a ∥ alignment is not what would be expected if binary disruption is a major contributor to pulsar proper motions.

- Natal supernovae "kicks" would then seem to be the dominant mechanism behind pulsar proper motions, and these "kicks" are primarily directed ∥ to a pulsar's rotation axis.

- The orderly orientations of core polarization provide further demonstration of the the distinct character of core emission by contrast to conal radiation or other types not yet identified.

- That core radiation both is the primary (central, low altitude) radio-frequency emission we are able to detect and tends strongly to propagate as the extraordinary (X) mode provides major insights into the operation of the pulsar "engine". It must be tertiary to the high energy primary particle acceleration just above the polar cap. It reflects heavy

processing by the highly magnetized dense plasma within the polar flux tube above the polar cap in which electromagnetic waves cannot propagate. Therefore, it must originate at a somewhat higher altitude at which plasma wave coupling to the X mode first becomes possible.

These conclusions are important not only for understanding the origins of pulsar emission but also for supernova theory. Spin-aligned supernova "kicks" imply either rotation averaging of hydrodynamic "kicks" on timescales much longer that the natal spin period or a magnetic field driven mechanism.

Similarly, the orderly alignments have important implications for understanding the detailed characteristics of the emission from individual pulsars. As we saw in our study of pulsar B0329+54 (Mitra *et al* 2007), our ability to identify the X and O modes of the emission facilitates a much more physical interpretation.

Establishing that the primary core emission is X mode further enables us to distinguish the magnetic orientation of its two OPMs everywhere within a pulsar's profile and to pursue questions about the overall emission more physically. Or said differently, the identification of core-associated X-mode emission in the profile centers of triple or five-component profiles permits us to identify the X/O character of the two conal-associated OPMs.

This all said, our largely average-polarimetry based analysis above remains the result of a rough tool. Our facilitating insights have come from the few available pulse-sequence polarization studies, and very much remains to be learned from such investigations of other pulsars. As regards core emission, its mechanisms and dynamics will be revealed through broad band polarimetric studies of its depolarization.

While we have been fairly successful in identifying core features on the basis of their geometry, spectral behavior and circular polarization, their linear polarization properties are highly variable. A few are highly polarized, but many are not, some are unimodal in form and other show bifurcation or a leading "pedestal" feature. In view of these varying characteristics, again it is surprising that the distribution of alignments is as strongly orthogonal as we have seen in Fig. 4. In particular, the "parent" core emission is not always dominant or is conflated with other profile features so is not easy to identify. Thus further study may well show that some of the 0° alignments represent O-mode emission rather than the "parent" X-mode radiation.

Again, we emphasize that these alignments are on the sky, as we have no direct means of considering the radial components of pulsar velocities. Given, however, the surprisingly compact distribution of transverse alignments, it is hard to imagine that the radial alignments could have a very different distribution. The effect of the unknown radial velocity components can be modeled statistically as Noutsos *et al* (2012) have done, and their overall conclusion to the above effect suggests that a detailed statistical modeling is unnecessary to support the results here.

It is interesting to look closely at those pulsars showing $\parallel$ or oblique alignments. Regarding the latter, some undoubtedly are cases like B1237+25 and B1508+55 where their positions on the sky are such that our lack of the radial velocity component is crucial—and the Ψ values thus misleading. Several other pulsars undoubtedly remain misclassified, for instance because core ($\mathbf{S}_t$) and conal single ($\mathbf{S}_d$) profiles can sometimes be difficult to distinguish.

The overall implication of our interpretation is that the fundamental curvature emission drives longitudinal plasma oscillations in the dense inner plasma of the polar flux tube (*e.g.*, Lyubarsky 2002). These plasma oscillations then first couple to X-mode radiation which often then seems to be converted into the O mode at higher altitude in an intensity-dependent manner. The plasma oscillations may well be responsible for the "bunching" needed for pulsars to radiate mainly at radio frequencies, and the consistent characteristic dimensions of core components probably follows from the non-refractiveness of the X mode.

Acknowledgments: The author thanks the anonymous referee and also Alice Harding, Aris Noutsos, Dipanjan Mitra and Paul Demorest for helpful suggestions on the analysis and manuscript. Portions of this work were supported by US NSF grants 08-07691 and 09-68296. Arecibo Observatory is operated by SRI International under a cooperative agreement with the NSF, and in alliance with Ana G. Méndez-Universidad Metropolitana, and the Universities Space Research Association. This research has made use of NASA's Astrophysics Data System.

REFERENCES

Backer, D. C., & Rankin, J. M. 1980, *Ap.J. Suppl.*, 42, 143
Bailes, M., Manchester, R. N., Kesteven, M. J., Norris, R. P., & Reynolds, J. E. 1990a, Nature, 343, 240
—. 1990b, M.N.R.A.S., 247, 322
Blaskiewicz, M., Cordes, J. M., & Wasserman, I. 1991, Ap.J., 370, 643
Brisken, W. F., Benson, J. M., Goss, W. M., & Thorsett, S. E. 2002, Ap.J., 571, 906
Brisken, W. F., Fruchter, A. S., Goss, W. M., Herrnstein, R. M., & Thorsett, S. E. 2003, A.J., 126, 3090
Chatterjee, S., Cordes, J. M., Lazio, T. J. W., et al. 2001, Ap.J., 550, 287
Chatterjee, S., Vlemmings, W. H. T., Brisken, W. F., et al. 2005, ApJ, 630, L61
Chatterjee, S., Brisken, W. F., Vlemmings, W. H. T., et al. 2009, Ap.J., 698, 250
Dodson, R., Legge, D., Reynolds, J. E., & McCulloch, P. M. 2003, Ap.J., 596, 1137
Fomalont, E. B., Goss, W. M., Manchester, R. N., & Lyne, A. G. 1997, M.N.R.A.S., 286, 81
Force, M. M., Demorest, P., & Rankin, J. M. preprint
Gott, III, J. R., Gunn, J. E., & Ostriker, J. P. 1970, ApJ, 160, L91
Gould, D. M., & Lyne, A. G. 1998, M.N.R.A.S., 301, 235
Harrison, P. A., Lyne, A. G., & Anderson, B. 1993, M.N.R.A.S., 261, 113
Helfand, D. J., Gotthelf, E. V., & Halpern, J. P. 2001, Ap.J., 556, 380
Hobbs, G., Lorimer, D. R., Lyne, A. G., & Kramer, M. 2005, M.N.R.A.S., 360, 974
Hobbs, G., Lyne, A. G., Kramer, M., Martin, C. E., & Jordan, C. 2004, M.N.R.A.S., 353, 1311
Johnston, S., Hobbs, G., Vigeland, S., et al. 2005, M.N.R.A.S., 364, 1397
Johnston, S., Kramer, M., Karastergiou, A., et al. 2007, M.N.R.A.S., 381, 1625
Karastergiou, A., & Johnston, S. 2006, M.N.R.A.S., 365, 353
Krishnamohan, S., & Downs, G. S. 1983, Ap.J., 265, 372
Lyne, A. G., Anderson, B., & Salter, M. J. 1982, M.N.R.A.S., 201, 503
Lyubarsky, Y. E. 2002, in Neutron Stars, Pulsars, and Supernova Remnants, ed. W. Becker, H. Lesch, & J. Trümper, 230
Manchester, R. N., Taylor, J. H., & Huguenin, G. R. 1975, Ap.J., 196, 83
Mitra, D., & Rankin, J. M. 2011, Ap.J., 727, 92
Mitra, D., Rankin, J. M., & Gupta, Y. 2007, M.N.R.A.S., 379, 932

Morris, D., Graham, D. A., Sieber, W., Bartel, N., & Thomasson, P. 1981, A&A Suppl., 46, 421
Morris, D., Graham, D. A., Sieber, W., et al. 1979, A&A, 73, 46
Ng, C.-Y., & Romani, R. W. 2004, Ap.J., 601, 479
Noutsos, A., Kramer, M., Carr, P., & Johnston, S. 2012, M.N.R.A.S., 423, 2736
Noutsos, A., Schnitzeler, D. H. F. M., Keane, E. F., Kramer, M., & Johnston, S. 2013, M.N.R.A.S., 430, 2281
Radhakrishnan, V., & Cooke, D. J. 1969, Astrophys. Lett., 3, 225
Radhakrishnan, V., & Deshpande, A. A. 2001, A&A, 379, 551
Rankin, J. M. 1983, Ap.J., 274, 333
—. 1990, Ap.J., 352, 247
—. 1993a, Ap.J., 405, 285
—. 1993b, *Ap.J. Suppl.*, 85, 145
—. 2007, Ap.J., 664, 443
Rankin, J. M., Rodriguez, C., & Wright, G. A. E. 2006, M.N.R.A.S., 370, 673
Rankin, J. M., Stinebring, D. R., & Weisberg, J. M. 1989, Ap.J., 346, 869
Shklovskii, I. S. 1969, AZh, 46, 715
Smith, E., Rankin, J., & Mitra, D. 2013, M.N.R.A.S., 435, 1984
Suleimanova, S. A., Volodin, Y. V., & Shitov, Y. P. 1988, Soviet Ast., 32, 177
Tademaru, E., & Harrison, E. R. 1975, Nature, 254, 676
Weltevrede, P., Edwards, R. T., & Stappers, B. W. 2006, A&A, 445, 243
Weltevrede, P., Stappers, B. W., & Edwards, R. T. 2007, A&A, 469, 607
Xilouris, K. M., Rankin, J. M., Seiradakis, J. H., & Sieber, W. 1991, A&A, 241, 87
Zou, W. Z., Hobbs, G., Wang, N., et al. 2005, M.N.R.A.S., 362, 1189

Table A1
Fiducial Polarization Angles for Stars Studied by Johnson I.

Pulsar	Cl	P (s)	$\log(\tau)$ (yrs)	PA_0 (deg)	Method
B0628–28[a]	S_t	1.244	6.443	26(2)	RVM fit
B0833–45	S_t	0.0893	4.053	37(1)	RVM fit
B0919+06	T	0.4306	5.696	–77(10)	PPA geom.[b]
B1237+25	M	1.3824	7.358	–28(4)	traverse
B1426–66	T?	0.7854	6.652	–29(1)	RVM fit
B1449–64	S_t	0.1795	6.017	–57(0)	RVM fit
B1451–68	M	0.2634	7.628	–22(4)	RVM fit
B1642–03	S_t	0.3877	6.538	**89(8)**[c]	see text
B1706–16	T	0.6531	6.215	**–75(2)**[c]	see text
B1706–44	S_t	0.1025	4.243	71(10)	Paper I
B1737+13	M	0.8031	6.943	–46(4)	RVM fit
B1842+14	T	0.3755	6.502	–52(2)	RVM fit
B1857–26	M	0.6122	7.676	–69(10)	Paper I
B1911–04	S_t	0.8259	6.508	–99(8)	Paper I
B1929+10	T	0.2265	6.491	–11(0)	RVM fit
B1933+16	T	0.3587	5.976	**–87(1)**[d]	see text

[a] ET VI classified this star as a conal (S_d) profile, but newer information now tilts toward its being a S_t star. Like B0823+26, it shows neither profile bifurcation nor conal outriders. [b] See Rankin et al. (2006) [c] The pulsar's latest core emission is polarized along a "track" that is ⊥ to the PM direction at the profile peak. See text.
[d] Here the underlying SPM PPA sweep is clearly seen only prior to about –7° longitude and in the tailing core region near +5-7°—and connecting the two shows the main regions of PPM power under the main peak and in the –6 to –3° interval. Connecting the former gives and intercept of about –87° at the primary profile peak. See the text.

Table A2
Fiducial Polarization Angles for Stars Studied in Paper I.

Pulsar	Cl	P (s)	$\log(\tau)$ (yrs)	PA_0 (deg)	Method
B0329+54	T/M	0.7145	6.743	20(4)	PPA geom.
B0355+54	S_t	0.1564	5.751	–41(4)	PPA geom.
B0450+55	T	0.3407	6.358	–23(16)[a]	PPA geom.
B0736–40	T	0.3749	6.566	–44(5)	PPA geom.
B0823+26	S_t	0.5307	6.692	48(3)	PPA geom.
B1508+55	T	0.7397	6.369	5(4)	PPA geom.

[a] Both Xilouris *et al* (1991) and recently Noutsos *et al* (2012) provide absolute polarimetry and in neither is the central PPA rotation resolved; however, the 327-MHz polarimetry in ET IX as well as that of Gould & Lyne (1998) and Suleimanova et al. (1988) show that the PPA rotates negatively though about 140°. Moreover, strong A/R effects in this pulsar were documented in ET IX from which it is clear that the fiducial longitude lags the central core by some 13°. Therefore a reasonable estimate of the PPA at the fiducial longitude PA_0 is about –23°.

APPENDIX

APPENDIX: RESULTS FOR INDIVIDUAL PULSARS

JOHNSTON I AND PAPER I VALUES

Of the 25 pulsars analyzed by Johnston *et al* (2006, Johnston I) and then reanalyzed by Rankin (2007, Paper I), 16 appear in Table A1 by virtue (with one exception) of their earlier classification in ET IV and/or ET VIb as having a core emission component. Apart from pulsar B1237+25, they all exhibit alignments $\Psi = PA_V - PA_0$ of close to 90°. The alignment values for B1642–03, B1706–16 and B1933+16 have been reinterpreted here as we have discussed above. They are given in boldface and differ from the values in Paper I in a similar manner as explained below.

These and several other core-dominated pulsars in Johnston I (*e.g.*, B1426–66 and B1451–68) share the common properties of distorted PPA traverses and highly depolarized profiles. In Paper I we appealed to observations at other (often lower) frequencies to more reliably interpret these PPA traverses. Now, dynamical studies of two similar pulsars [B0329+54 (Mitra *et al* (2007) and B1237+25 (Smith *et al* (2013)] have helped us understand how this distortion and depolarization occurs systematically. Single mode emission in the trailing parts of a core component also appears earlier because of intensity-dependent aberration/retardation, and in some cases it seems to undergo conversion to the other mode. A relatively straightforward such case is shown for pulsar B1706–16 in Figure 2, where overall the emission in the two OPMs follows a negative-going, nearly linear PPA traverse. Here and in other cases, this later core emission (not that of any trailing conal outrider) is relatively undistorted by the intensity-dependent A/R and consequent depolarization through OPM mixing, so we use this later OPM to estimate the "fiducial" PPA. Clearly core emission entails a variety of core properties wherein for Vela and most other pulsars in Table A1 the dominant (or later "parent") emission is ⊥ to the PM PA_v direction and thus to **B**; whereas in other cases complex depolarization occurs and/or the secondary, apparently converted OPM becomes dominant at the fiducial longitude.

Paper I also studied pulsars using the absolute polarimetry from Morris *et al* (1979, 1981), Xilouris *et al* (1991) and Karastergiou & Johnston (2006). Of the 21 such stars in Paper I, 6 appear in Table A2 below again by virtue of their classification among one of the three profile groups having core components in ET IV or VIb. For these prominent and well studied pulsars, the PPA traverse geometry is usually well understood from mul-

Table A3
Fiducial Polarization Angles for Stars Studied by Johnson II.

Pulsar	Cl	P (s)	log(τ) (yrs)	PA_0 (deg)	Method
B0450–18[a]	T	0.5489	6.179	47(3)	RVM fit
B0540+23[b]	S_t	0.2460	5.403	–85(3)[c]	RVM fit
B0835–41	S_t	0.7516	6.526	–84(5)	RVM fit
B1600–49	T?	0.3274	6.707	0(5)[d]	V zero
B1818–04	T	0.5981	6.176	55(3)[e]	PPA geom.
B1848+13	S_t?	0.3456	6.565	–45(3)	RVM fit
B1913+10	S_t	0.4045	5.623	85(3)	RVM fit
B1935+25	S_t	0.2010	6.695	–56(8)[f]	PPA geom.
B2045–16	T	1.9616	6.453	–13(5)	RVM fit
B2327–20	T	1.6436	6.750	21(10)	RVM fit

[a] This pulsar needs study at a single pulse level. Johnston II's 3.1-GHz and and 691-MHz profiles seem from different stars—and the smooth high frequency PPA traverse is deceptive; most lower frequency profiles show multiple L minima and 90° "jumps"—possibly due to A/R effects.
[b]Long classified as $\mathbf{S}_t$, the asymmetry of the PPA inflection and lack of outriders cast this classification into serious doubt.
[c] BCW's fiducial PPA longitude falls 18° after the peak.
[d]Fiducial longitude taken at the V zero-crossing point.
[e]The high frequency core center provides a better fiducial longitude.
[f]This pulsar's leading component is a highly polarized precursor, and the second feature appears to have a core-single profile. Thus we take the fiducial longitude at what seems to be the core peak at 3.1 GHz. The 691-MHz profile is so depolarized in this region that no reliable PPAs can be measured.

Table A4
Fiducial Polarization Angles from Force *et al* (2015).

Pulsar	Cl	P (s)	log(τ) (yrs)	PA_0 (deg)	Method
B0011+47	T?	1.2407	7.542	43(7)	RVM fit
B0136+57[a]	S_t	0.2725	5.605	43(3)	RVM fit
B1322+83	S_t	0.6700	7.272	26(3)	PPA geom.
B1732–07	T	0.4193	6.738	–22(1)[b]	RVM fit
B1821–19	S_t?	0.1893	5.758	53(2)	RVM fit
B1826–17	T?	0.3071	5.943	11(1)	RVM fit
B2111+46	T	1.0147	7.352	86(0)	RVM fit
B2217+47	S_t	0.5385	6.490	65(8)	RVM fit
B2224+65	S_t	0.6825	6.049	–48(5)	ET IX,X
B2255+58	S_t	0.3682	6.004	24(3)	RVM fit
B2310+42	M	0.3494	7.693	18(10)	RVM fit

[a] ET VIb classified this star as having an $\mathbf{S}_t$ profile, but Weltevrede et al. (2006, 2007) find weak evidence of drifting. Neither conal outriders nor low frequency bifurcation has been seen—so the classification is uncertain. The PPA rotation in Noutsos *et al* (2012) seems to have the incorrect sense.
[b]Fitted steep central PPA traverse unresolved in Johnston II.

Table A5
Fiducial Polarization Angles from this paper.

Pulsar	Cl	P (s)	log(τ) (yrs)	PA_0 (deg)	Method
B1541+09	T	0.7484	7.438	–32(15)	PPA geom.
B1946+35[a]	S_t	0.7173	6.207	–78(15)	PPA geom.
B2053+36	S_t	0.2215	6.978	–77(11)	PPA geom.
B2110+27	S_t	1.2028	6.861	–64(5)	PPA geom.

[a]Single-pulse polarimetry study is needed to reliably interpret this pulsar's complex and depolarized profile in the core region.

tiple sources. Most of these PA_0 values are identical to those in Paper I; however, the PA_0 values for B0450+55 has been reinterpreted on the basis of new information.

Johnston II, Force et al, and AO Values

A further major source of fiducial PA_0 values is Johnston *et al* (2007, Johnston II), and these appear in Table A3. Of the 22 pulsars in the foregoing paper, 10 appear here, and most were classified as above or in ET IX. Overall this group is less well studied in terms of profile geometry, often because polarimetric observations are available only at one or two frequencies. Notes show how the pulsars were interpreted here when the resulting PA_0 values differ from those in Johnston II.

Force *et al* (2015) conducted absolute polarimetric measures with the Green Bank Telescope. Of the 33 Force *et al* stars, 11 with clear or probable core components appear in Table A4. Again, this group has been less well studied in terms of profile geometry, often because their weakness makes observations over a broad band difficult.

Finally, we report four values from Arecibo measurements in this paper. These used four Mock Spectrometers (www.naic.edu/∼astro/mock.shtml) sampling bands of 86 MHz centered at 1270, 1420, 1520 and 1620 MHz with milliperiod sampling. The resulting polarized profiles were derotated to infinite frequency are shown in Fig. A1. All reference nominal 21-cm observations (by averaging the bottom three bands), and they entail straightforward interpretations in that their fiducial longitudes fall very close to the central component peaks. Their PA_0 values are given in Table A5.

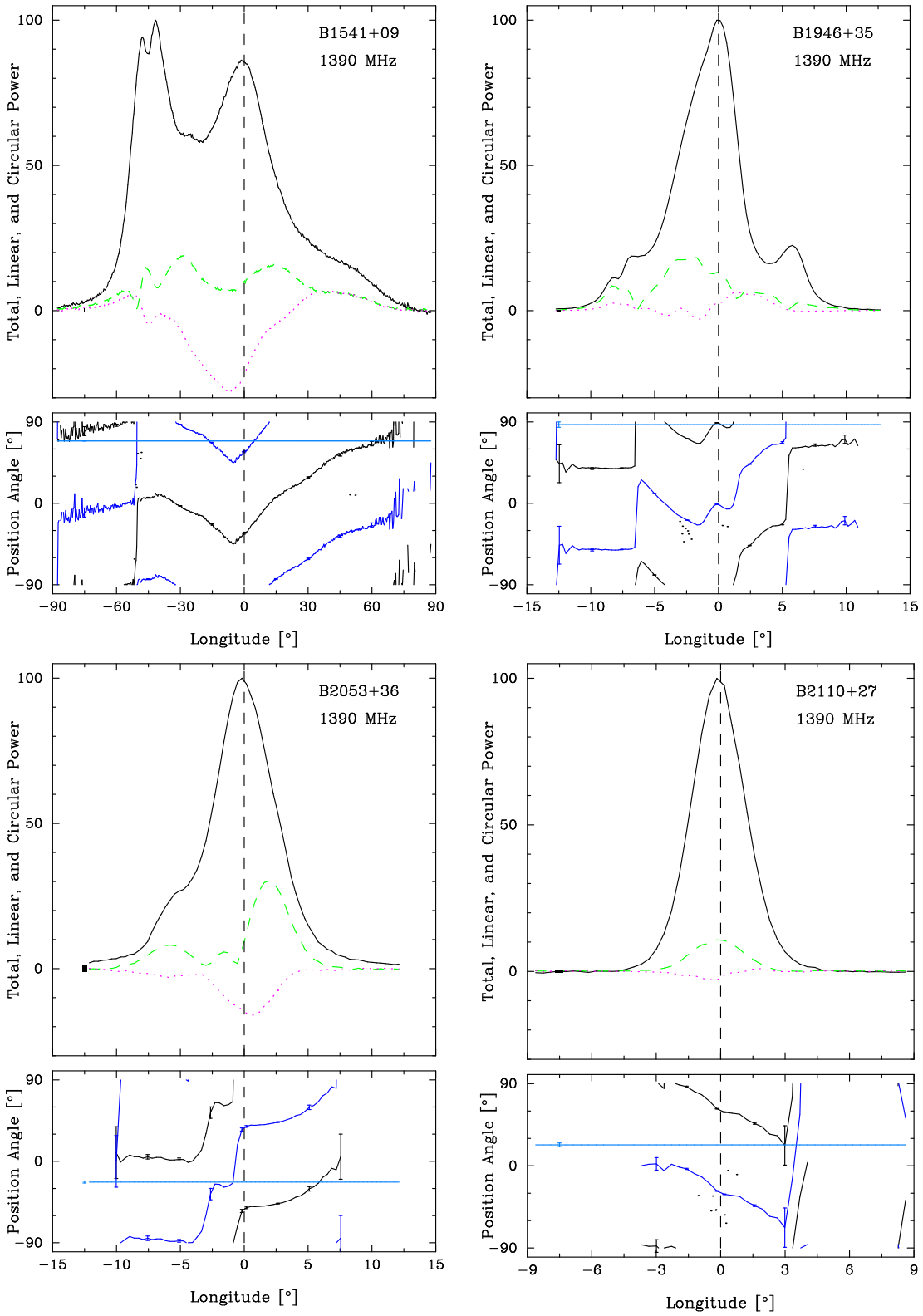


Figure A1. Polarization profiles for B1541+09, B1946+35, B2053+36 and B2110+27. Here the total power (black), total linear polarization (green dashed) and circular polarization (magenta dotted) are plotted in the upper panels. The Faraday derotated PPA information (black) is plotted in the lower panels and the PPA–90° (blue) is also shown along with bars indicating the errors. Finally, a cyan line shows the PA_V value.